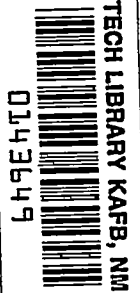


NACA RM L55L20a



NACA

RESEARCH MEMORANDUM

Rep # 15-65-5

2 11 1956

FACTORS AFFECTING THE MAXIMUM LIFT-DRAG RATIO
AT HIGH SUPERSONIC SPEEDS

By Charles H. McLellan and Robert W. Dunning

Langley Aeronautical Laboratory
Langley Field, Va.

CLASSIFIED DOCUMENT

NATIONAL ADVISORY COMMITTEE
FOR AERONAUTICS

WASHINGTON

February 13, 1956

Classification requested (or changed to) Unclassified
By Author: NASA Tech Pub Arrangement #29
(ORIGINAL AUTHORIZED TO CHANGE)

By: 27 Sept 68

OK

GRADE 01

7 Apr 61
DATE



NATIONAL ADVISORY COMMITTEE FOR AERONAUTICS

RESEARCH MEMORANDUM

FACTORS AFFECTING THE MAXIMUM LIFT-DRAG RATIO

AT HIGH SUPERSONIC SPEEDS

By Charles H. McLellan and Robert W. Dunning

SUMMARY

A study of the factors affecting the maximum lift-drag ratio $(L/D)_{MAX}$ has been conducted in an effort to determine how to obtain high aerodynamic $(L/D)_{MAX}$ values at high supersonic Mach numbers. Wings, bodies, and wing-body combinations are discussed, and some of the effects of leading-edge heating on wing geometry and $(L/D)_{MAX}$ are included. It appears hopeful that high $(L/D)_{MAX}$ values may be achieved at the high supersonic Mach numbers by utilization of as high a Reynolds number laminar flow as possible, low-aspect-ratio wings, favorable interference effects, and the use of more radical configurations.

INTRODUCTION

At high supersonic speeds the importance of maintaining high values of maximum lift-drag ratio $(L/D)_{MAX}$ in long-range vehicles is essentially the same as at low speeds (refs. 1, 2, and 3). The range is primarily a function of the lift-drag ratio and the ratio of fuel weight to gross weight. At very high speeds, the centrifugal forces also affect the range; however, in the present paper only the aerodynamic $(L/D)_{MAX}$ will be considered. As at low speeds, $(L/D)_{MAX}$ should not be increased at the expense of excessive structural weight. Compared with the lower speed ranges, the problem of obtaining high lift-drag ratios at very high supersonic speeds is a relatively unexplored field requiring much further investigation. It is the purpose of this paper to examine some of the more important factors affecting $(L/D)_{MAX}$.

SYMBOLS

R	Reynolds number
M	Mach number
L/D	lift-drag ratio
W/S	wing loading, lb/sq ft
S	wing area
T	temperature
t/c	ratio of wing thickness to chord
A	wing aspect ratio
ϵ	emissivity
Λ	leading-edge sweepback, deg
q	heat transfer, Btu/hr

Subscripts:

MAX	maximum
L.E.	leading edge
W	wing

DISCUSSION

The skin friction, and, therefore, Reynolds number, is a major factor and will be discussed first. For an airplane operating at its $(L/D)_{MAX}$ the Reynolds number will be determined by the wing loading, $(L/D)_{MAX}$, and Mach number. Figure 1 shows the probable range of Reynolds number per foot for high-speed configurations operating at $(L/D)_{MAX}$. The upper limit is defined by a high wing loading and a high aerodynamic $(L/D)_{MAX}$, whereas the lower limit is defined by a low wing loading and a low $(L/D)_{MAX}$. In figure 1 this upper limit has been chosen arbitrarily as having an $(L/D)_{MAX}$ of 6 and a wing loading of 100 pounds per square foot, and the lower limit as having an $(L/D)_{MAX}$ of 2 and a wing loading

of 10 pounds per square foot. With moderate wing loadings, $(L/D)_{MAX}$ will be reached at altitudes between 100,000 and 200,000 feet for the high supersonic speeds. At these altitudes the Reynolds number will be relatively low (ref. 4) (on the order of 1×10^6 to 10×10^6 on a 10-foot chord) and, on the basis of current research data, it appears hopeful that laminar flow can be maintained over much of the configuration (refs. 5 and 6 and unpublished data obtained in the Langley 11-inch hypersonic tunnel and in the Ames free-flight tunnel).

The effect of Reynolds number on $(L/D)_{MAX}$ as the Mach number is increased is presented in figure 2 for the simplest possible case of the two-dimensional flat plate. With a laminar boundary layer at a Reynolds number of 1×10^6 , $(L/D)_{MAX}$ decreases with Mach number until it reaches a nearly constant value of about 7 at Mach numbers of 10 and above. For a Reynolds number of 10×10^6 , the shape of the curve is the same as at 1×10^6 ; however, $(L/D)_{MAX}$ is higher, being on the order of 12 at Mach numbers above 10. As expected, the turbulent boundary layer gives values well below those of the laminar boundary layer for the lower Mach numbers; however, at the very high Mach numbers, $(L/D)_{MAX}$ is approaching the laminar values. A 10° cone and an infinite cylinder at a Reynolds number of 1×10^6 , which are shown for comparison with the flat plate, have relatively low values of $(L/D)_{MAX}$, and it becomes obvious that the wing should be as big as practical with respect to the body to obtain the highest $(L/D)_{MAX}$. In addition, the Reynolds number should be as high as possible without causing boundary-layer transition.

Of course, a more realistic evaluation of wings requires consideration of the effects of thickness. At high Mach numbers, a flat lower surface and a thin nose angle are desirable (ref. 7), and this can best be obtained in a wedge airfoil. Figure 3 shows the calculated effect of thickness on wedge airfoil sections of infinite-span wings at a Mach number of 7. At the low thicknesses, the upper surface is shielded from the free-stream flow; and as the thickness increased to about 0.07 at $R = 1 \times 10^6$ and 0.04 at $R = 1 \times 10^7$, the upper surface becomes parallel to the free stream at $(L/D)_{MAX}$. Beyond this point, the upper surface is exposed to the stream. It is sometimes supposed that, at high supersonic Mach numbers, thickness can be added to the upper surface in the shielded region without affecting $(L/D)_{MAX}$. It can be seen that even partially filling in the shielded area results in loss in $(L/D)_{MAX}$ at this Mach number. Similar effects can be anticipated for other wing sections.

Another factor affecting $(L/D)_{MAX}$ is the aspect ratio. As pointed out previously, the Reynolds number should be as great as is consistent with the maintenance of laminar flow. Early in the design of a configuration the wing area and operating conditions will probably be fixed. With a fixed-wing area, and operating conditions, the Reynolds number can be increased by decreasing the aspect ratio. Figure 4 shows the variation of $(L/D)_{MAX}$ with aspect ratio for a constant-area rectangular wing with a sharp-leading-edge symmetrical double-wedge section at a Mach number of 7. As the aspect ratio decreases, the wing chord and, consequently, the Reynolds number increase, and the skin friction decreases. Without tip effects, $(L/D)_{MAX}$ would continually increase with decreasing aspect ratio. The tip losses, however, reduce $(L/D)_{MAX}$ more at the low aspect ratios so that, theoretically, a maximum is reached in this particular case at an aspect ratio of about 0.6. The two experimental points appear to agree with this trend even though the section was slightly different for the low-aspect-ratio wing. (A 5-percent-thick symmetrical double-wedge section would be slightly lower.) At higher Mach numbers, the optimum aspect ratios would be smaller. The decrease in aspect ratio will probably reduce the structural thickness requirements and will allow thinner sections to be used, which will increase the values of $(L/D)_{MAX}$.

A similar effect would be expected for triangular plan-form wings. In figure 5, $(L/D)_{MAX}$ at $M = 7$ has been plotted against aspect ratio for the same airfoil section and constant wing area for a family of triangular wings with a laminar boundary layer. The calculated curve is for the region with attached shock where the lift-curve slope and wave drag are constant (ref. 8). The change in estimated $(L/D)_{MAX}$ results from the change in skin friction.


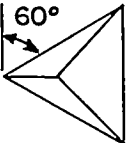
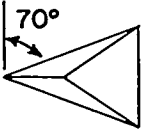
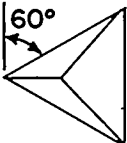
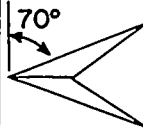
The experimental points seem to verify the theoretical trend. However, in all the experimental work at this Mach number in the Langley 11-inch hypersonic tunnel, the values of $(L/D)_{MAX}$ are lower than the theoretical ones. Because of the so-called shock-boundary-layer interaction, the experimental minimum drag is considerably greater than the predicted drag. At the Mach number and Reynolds number of this investigation, the boundary layer displaces the flow about the wing (ref. 9), resulting in increased pressure which increases the skin friction for the two-dimensional case by about 20 percent. Higher Reynolds numbers will decrease this effect, whereas higher Mach numbers will increase it. As can be seen from figures 4 and 5, there appears to be little difference either theoretically or experimentally between the rectangular wing and the triangular wing of the same aspect ratio, and it would appear that either low-aspect-ratio rectangular wings or very highly swept triangular wings will give the highest values of $(L/D)_{MAX}$. The sweep should not be increased or the aspect ratio decreased to the point where

the Reynolds number becomes so high that transition occurs on the wing. Theoretical and experimental results (refs. 10 and 11) indicate that transition occurs earlier with a swept leading edge than with an unswept leading edge. Therefore, higher Reynolds number laminar flow can probably be obtained on rectangular wings than on triangular ones. Furthermore, for the same average Reynolds number, a triangular wing will have a root-chord Reynolds number twice that of the rectangular wing so that transition would be expected at a lower average Reynolds number on the triangular wing. It should also be noted that the triangular wing $(L/D)_{MAX}$ could probably be improved by removing some of the low Reynolds number high-drag tip.

In the high Mach number range, the problem of aerodynamic heating of the leading edge will also enter into the choice of the wing plan form. The highly swept wings have an advantage in that the heat transfer per unit area to a blunt leading edge decreases with leading-edge sweep (refs. 12 and 13) and allows the use of smaller leading-edge diameters. Furthermore, as is well known, the drag of a blunt leading edge decreases with sweep angle (refs. 14 and 15). Therefore, the use of sweep would be expected to decrease not only the required leading-edge diameter but also the loss in $(L/D)_{MAX}$ due to a given leading-edge bluntness. If radiant cooling is used, the diameter required is a function of both Mach number and sweep angle. Figure 6 presents the diameter required for an arbitrary leading-edge equilibrium temperature of $2,500^{\circ}\text{F}$ with a surface ϵ of 0.8 and at altitudes of interest at the high Mach numbers. Materials are available for use as leading edges which can be operated at this and possibly even greater temperatures. Below $M = 6$, the recovery temperature is below the $2,500^{\circ}\text{F}$ limit; and a sharp leading edge could be used with this temperature limit and sweep would not be necessary from the standpoint of leading-edge heating. With small leading-edge sweeps, the diameter required increases very rapidly for both the 100,000- and 150,000-foot altitudes as the Mach number is increased above 6. The large sweep angles greatly decrease the required diameter; however, even with large sweep angles, the diameters become very large, on the order of several inches at high Mach numbers, and some other means of cooling may be required.

Since blunted leading edges may be required at the higher Mach numbers, it is of interest to examine their effects on $(L/D)_{MAX}$. As an illustration, figure 7 has been prepared for a 400-square-foot wing at an altitude of 120,000 feet when flying at a Mach number of 11. At lower Mach numbers, the curves are similar to this one. Increasing the sweep increases $(L/D)_{MAX}$ particularly for the large leading-edge diameters. The aspect-ratio-0.3 rectangular wing is about the same as the 60° triangular wing. Except at the very small leading-edge diameters, the 70° swept wing has the highest $(L/D)_{MAX}$.

Since the leading-edge diameter required for radiant cooling decreases rapidly with high sweep angles, the high sweep angles would be preferred for the radiant-cooling case. High sweep, however, may not be necessary or even desirable if some means of forced cooling, such as transpiration cooling, is employed, since the total heat to the leading edge is important. This is illustrated in the following table which presents effects of wing plan form on $(L/D)_{MAX}$ with both forced and radiant cooling for the same conditions as figure 7 for laminar boundary layer and $M = 11$, $S = 400$ square feet, and an altitude of 120,000 feet:

	Forced cooling, $T_{L.E.} = 212^{\circ} F^a$			Radiant cooling, $T_{L.E.} = 2,500^{\circ} F^a$, $\epsilon = 0.8^a$	
	 $A = 0.3$	 60°	 70°	 60°	 70°
L.E. diam., in.	^a 0.5	^a 0.5	^a 0.5	6.7	3.0
q , Btu $\times 10^6$ /hr	.79	2.05	1.61	5.64	2.98
$(L/D)_{MAX}$	6.4	6.3	7.0	2.9	5.4

^aAssumed value.

The leading-edge diameter should be kept as small as practical with a forced cooling system. For this analysis, a 1/2-inch diameter has been assumed. The rectangular wing with forced cooling would have an $(L/D)_{MAX}$ value of 6.4 and would have a heat transfer to the leading edge of less than 1 million Btu's per hour. This could be absorbed by evaporating less than 1,000 pounds of water per hour. The 60° wing would have about the same $(L/D)_{MAX}$, but because of its greater wing span would have nearly three times the amount of heat to be absorbed. The 70° wing would have a higher $(L/D)_{MAX}$ but would have over twice the amount of heat to be absorbed as the rectangular wing. Furthermore, the cooling system would be spread out over a long leading edge requiring more plumbing. Therefore, for forced cooling, the very low-aspect-ratio rectangular wings appear desirable.

For the radiant-cooled leading edge, $(L/D)_{MAX}$ would be very low on the 60° wing because of the large leading edge required. Even the 70° wing requires a 3-inch leading-edge diameter and has a value of $(L/D)_{MAX}$ of only 5.4. The loss in $(L/D)_{MAX}$ probably would not be

quite as great in an actual application since the wings with low $(L/D)_{MAX}$ should be operated at a higher altitude than for those with high $(L/D)_{MAX}$. However, this is a secondary effect which has been neglected. Still larger sweep angles would probably be desirable with radiant cooling.

From the foregoing discussion, both the highly swept triangular wings and the low-aspect-ratio rectangular wings begin to appear like thin bodies, suggesting that the bodies should probably be shaped somewhat like thick wings. Bodies, however, have been discussed extensively in the past (for example, refs. 16 and 17) and will, therefore, be discussed only briefly. Figure 8 shows the general trend of increasing $(L/D)_{MAX}$ as the bodies take on more of a wing-like shape. The bodies in order of the increasing $(L/D)_{MAX}$ are the 20° cone cylinder, the 10° cone cylinder, a drooped-nose flat-bottomed model with the upper surface of the nose approximately filling in the lee side at $(L/D)_{MAX}$, and the upper body in which the aspect ratio has been doubled. These bodies are discussed more extensively in reference 16. The aspect ratios are below the optimum for the flat-bottomed bodies, and a considerable penalty is being paid for filling in the lee side. A thin wing with nearly the same plan form and Reynolds number had an $(L/D)_{MAX}$ of about 5.4 as compared with 4.4 for the best body in this figure.

The final object is to develop complete configurations with high $(L/D)_{MAX}$. At the high supersonic Mach numbers, configurations are still in the early stages of development. In figure 9, the estimated $(L/D)_{MAX}$ for two complete configurations is shown. These configurations, with the same body size, have rounded leading edges for radiant cooling for Mach numbers up to about 7 and provisions for obtaining stability. The calculations have been made for laminar flow at the altitude required for the given wing loadings and the lift coefficients at $(L/D)_{MAX}$.

The more or less conventional configuration with a trapezoidal wing shows the values of $(L/D)_{MAX}$ that can be expected from present-type aircraft. It utilizes wedge-shaped tail surfaces and can be expected to have good stability characteristics throughout the speed range as well as having a landing speed of only 150 knots. The value of $(L/D)_{MAX}$ with all laminar flow varies from 5 to about 4. With this wing loading of 50 pounds per square foot, $(L/D)_{MAX}$ was obtained at a Reynolds number of only 2×10^6 based on the mean aerodynamic chord, and laminar flow is likely over much of the configuration.

The three-wing configuration proposed in reference 3 to obtain high $(L/D)_{MAX}$ at high Mach numbers is also shown in figure 9. This configuration with laminar flow has an estimated value of $(L/D)_{MAX}$ between 5 and 6.

This relatively high value of $(L/D)_{MAX}$ results largely from the high wing area with respect to the body area, and to the high Reynolds number. The high sweep decreases the leading-edge drag, but the large surface area of the nonlifting upper wing increases the skin-friction drag of the configuration. The negative dihedral is included for the low-speed stability and decreases the value of $(L/D)_{MAX}$ according to unpublished wind-tunnel tests at Mach numbers from 3 to 6 in the Ames 10- by 14-inch tunnel.

In order to obtain higher values of $(L/D)_{MAX}$, more radical configurations should be considered. One possibility is to combine the body and wing features into one. Figure 10 shows two such configurations. No provisions have been made for obtaining stability or cooling of the leading edge on these configurations. The volume normally obtained in a body is obtained by filling in part of the area above the lower surface on these configurations. A rectangular wedge-shaped configuration of aspect ratio 0.4 would have an estimated value of $(L/D)_{MAX}$ of 7 at $M = 3$ and of nearly 10 at $M = 12$. The Reynolds numbers are very high, 30×10^6 at $M = 10$, and transition might occur. The increased skin friction obtained by assuming fully turbulent flow reduced $(L/D)_{MAX}$ to between 6 and 7.

The configuration with a triangular plan form with clipped tips had the same body volume and wing area as the rectangular configuration. The value of $(L/D)_{MAX}$ with laminar flow was about the same for the two configurations. As pointed out previously, transition is more likely on the triangular-plan-form configurations at a given Reynolds number than with the rectangular one.

One factor involved in configuration development which needs to be investigated is that of interference effects between wings and bodies. Ferri, Clark, and Casaccio (ref. 18) have proposed the use of wedges under wings to generate a high-pressure region and thereby increase the lift. If a configuration can be designed so that existing high-pressure regions, such as that emanating from a body nose, are located under the wing, it should be possible to obtain increased values of $(L/D)_{MAX}$ as a result of the interference effects.

Figure 11 shows the results of some unpublished calculations by A. J. Eggers, Jr., and Clarence A. Syvertson of the Ames Aeronautical Laboratory for a highly swept zero-thickness wing in combination with a half-conical body. This curve shows $(L/D)_{MAX}$ for the wing alone, body under the wing, and body above the wing for laminar flow at a Mach number of 7. Putting the cone body on the bottom of the wing entailed much smaller losses than putting the cone body on the top because of the more

favorable interference effects of the high pressure from the low body on the wing. Preliminary unpublished experimental results seem to verify this trend. These interference effects are obviously very important and should be investigated further.

CONCLUDING REMARKS

In general, the study of how to obtain high aerodynamic values of maximum lift-drag ratio $(L/D)_{MAX}$ has indicated that configurations should be operated at as high a Reynolds number as possible, providing that the boundary layer remains laminar. Low-aspect-ratio rectangular wings appear to be best when small leading-edge diameters can be used as with transpiration cooling. When radiant cooling of the leading edge is used, a highly swept wing may be desirable. By utilization of favorable interference effects and the use of the more radical configurations, it appears hopeful that high values of $(L/D)_{MAX}$ may be achieved at the high supersonic Mach numbers.

Langley Aeronautical Laboratory,
National Advisory Committee for Aeronautics,
Langley Field, Va., November 3, 1955.

~~CONFIDENTIAL~~

REFERENCES

1. Sänger, Eugen: Raketen-Flugtechnik. R. Oldenbourg (Berlin), 1933.
2. Sänger, E., and Bredt, I.: A Rocket Drive for Long Range Bombers. Translation CGD-32, Tech. Information Branch, Bur. Aero., Navy Dept., Aug. 1944.
3. Seiff, Alvin, and Allen, H. Julian: Some Aspects of the Design of Hypersonic Boost-Glide Aircraft. NACA RM A55E26, 1955.
4. The Rocket Panel: Pressures, Densities, and Temperatures in the Upper Atmosphere. Phys. Rev., vol. 88, no. 5, Second ser., Dec. 1, 1952, pp. 1027-1032.
5. Korkegi, R. H.: Transition Studies and Skin Friction Measurements on an Insulated Flat Plate at a Hypersonic Mach Number. Memo. No. 17 (Contract No. DA-04-495-Ord-19), GALCIT, July 15, 1954.
6. Jedlicka, James R., Wilkins, Max E., and Seiff, Alvin: Experimental Determination of Boundary-Layer Transition on a Body of Revolution at $M = 3.5$. NACA TN 3342, 1954.
7. Chapman, Dean R.: Reduction of Profile Drag at Supersonic Velocities by the Use of Airfoil Sections Having a Blunt Trailing Edge. NACA RM A9H11, 1949.
8. Bertram, Mitchel H., and McCauley, William D.: An Investigation of the Aerodynamic Characteristics of Thin Delta Wings With a Symmetrical Double-Wedge Section at a Mach Number of 6.9. NACA RM L55B14, 1955.
9. Bertram, Mitchel H.: An Approximate Method for Determining the Displacement Effects and Viscous Drag of Laminar Boundary Layers in Two-Dimensional Hypersonic Flow. NACA TN 2773, 1952.
10. Stuart, J. T.: The Basic Theory of the Stability of Three-Dimensional Boundary-Layers. Rep. No. F.M. 1899, British N.P.L. (Rep. No. 15,904, A.R.C.), May 13, 1953.
11. Dunning, Robert W., and Ulmann, Edward F.: Effects of Sweep and Angle of Attack on Boundary-Layer Transition on Wings at Mach Number 4.04. NACA TN 3473, 1955.
12. Feller, William V.: Investigation of Equilibrium Temperatures and Average Laminar Heat-Transfer Coefficients for the Front Half of Swept Circular Cylinders at a Mach Number of 6.9. NACA RM L55F08a, 1955.

~~CONFIDENTIAL~~

13. Eggers, A. J., Jr., Hansen, C. Frederick, and Cunningham, Bernard E.: Theoretical and Experimental Investigation of the Effect of Yaw on Heat Transfer to Circular Cylinders in Hypersonic Flow. NACA RM A55E02, 1955.
14. Penland, Jim A.: Aerodynamic Characteristics of a Circular Cylinder at Mach Number 6.86 and Angles of Attack Up to 90° . NACA RM L54A14, 1954.
15. Jones, Robert T.: Effects of Sweep-Back on Boundary Layer and Separation. NACA Rep. 884, 1947. (Supersedes NACA TN 1402.)
16. Resnikoff, Meyer M.: Optimum Lifting Bodies at High Supersonic Airspeeds. NACA RM A54B15, 1954.
17. Ridyard, Herbert W.: The Aerodynamic Characteristics of Two Series of Lifting Bodies at Mach Number 6.86. NACA RM L54C15, 1954.
18. Ferri, Antonio, Clarke, Joseph H., and Casaccio, Anthony: Drag Reduction in Lifting Systems by Advantageous Use of Interference. PIBAL Rep. No. 272 (Contract AF 18(600)-694), May 1955.

PROBABLE AIRPLANE ENVIRONMENT

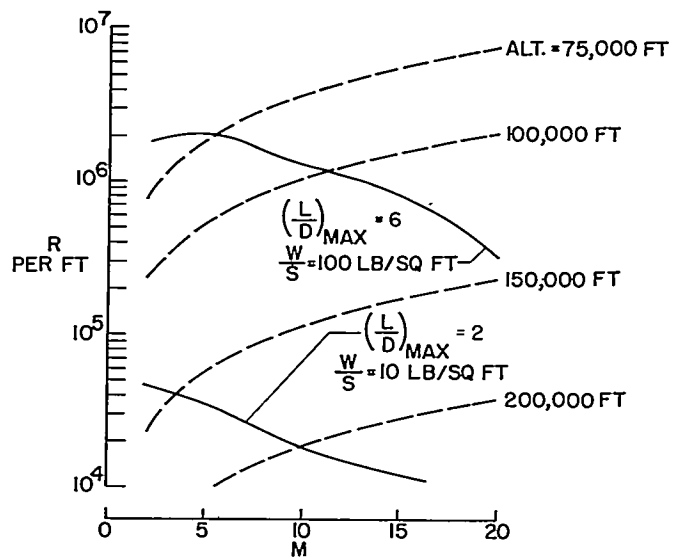
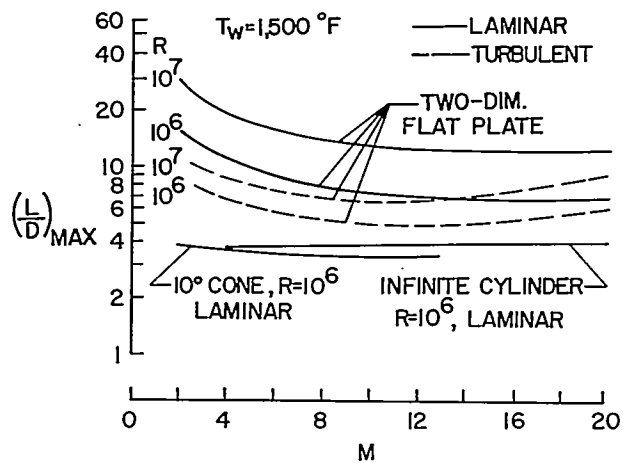


Figure 1

EFFECTS OF REYNOLDS NUMBER AND MACH NUMBER ON $(\frac{L}{D})_{MAX}$ 

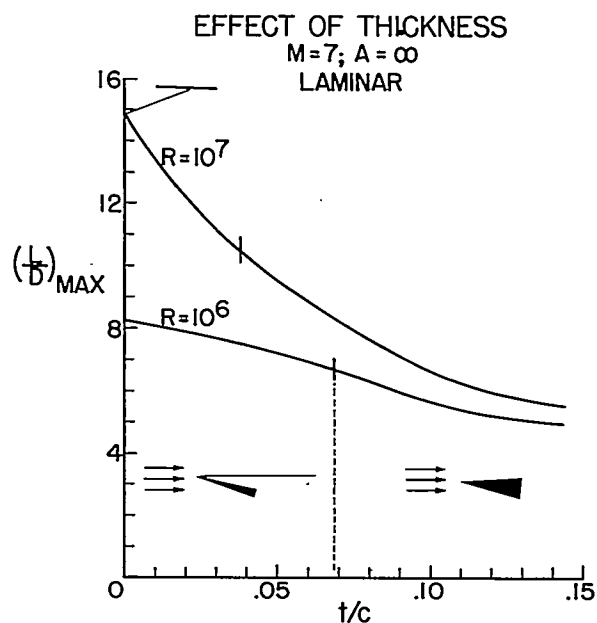


Figure 3

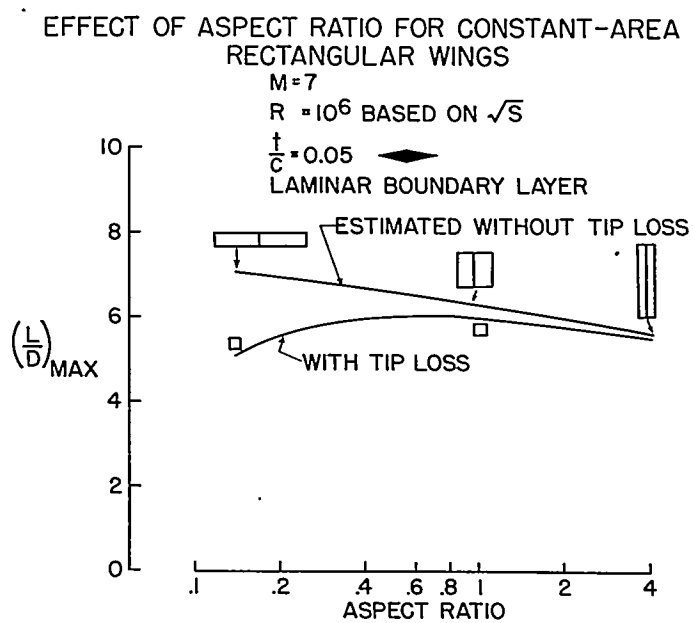


Figure 4

EFFECT OF ASPECT RATIO FOR CONSTANT-AREA TRIANGULAR WINGS

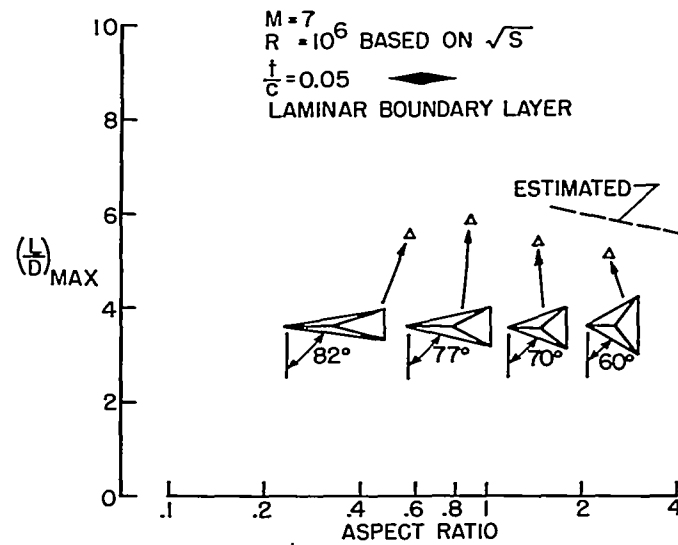


Figure 5

LEADING-EDGE DIAMETER REQUIRED FOR RADIANT COOLING

$T = 2500^\circ\text{F}$, $\epsilon = 0.8$
 LAMINAR

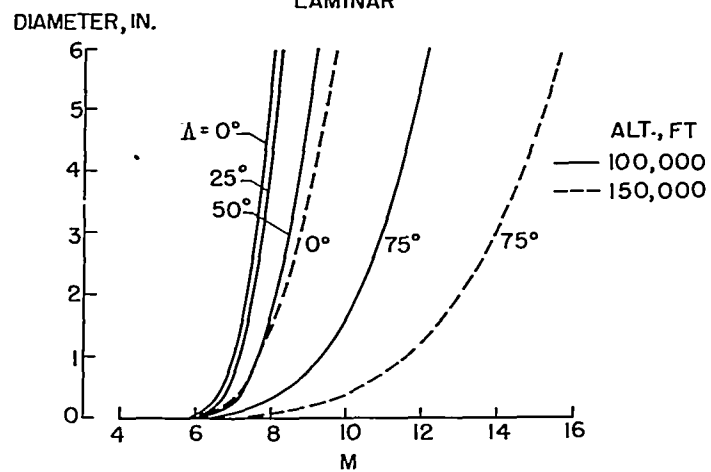


Figure 6

CONFIDENTIAL

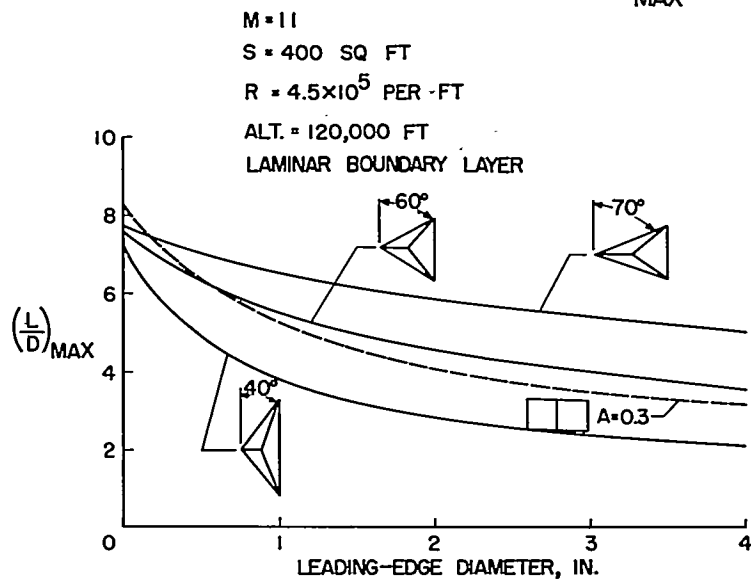
EFFECT OF LEADING-EDGE DIAMETER ON $(\frac{L}{D})_{MAX}$ 

Figure 7

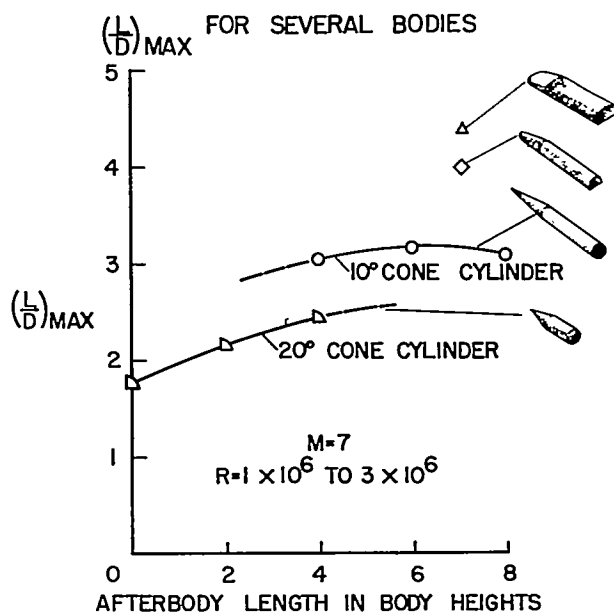


Figure 8

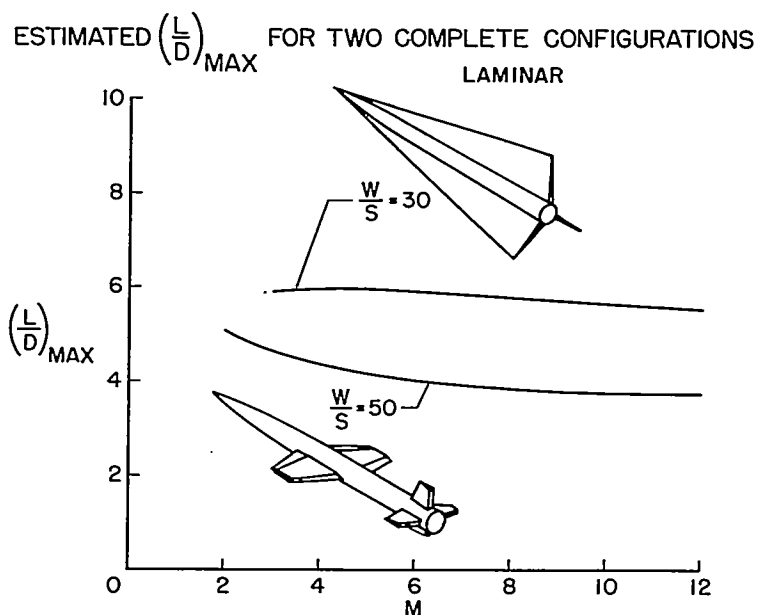


Figure 9

ESTIMATES FOR TWO HIGH $\left(\frac{L}{D}\right)_{\text{MAX}}$ CONFIGURATIONS
 $W/S = 30 \text{ LB/SQFT}$; $S = 600 \text{ SQFT}$

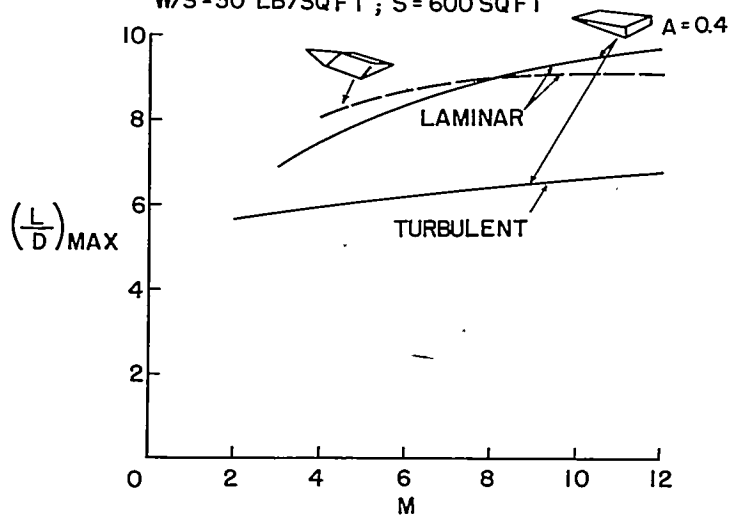


Figure 10

CONFIDENTIAL

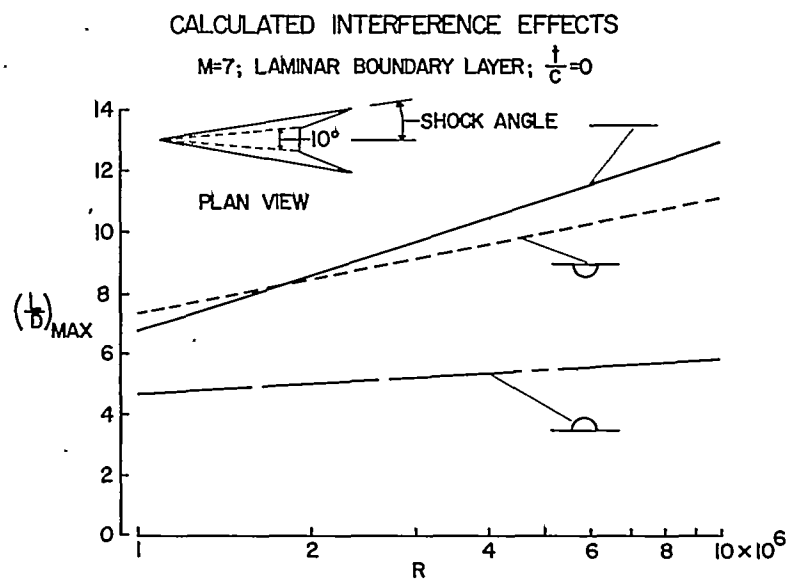


Figure 11